Fisher's zeros as boundary of RG flows in complex coupling space

Yannick Meurice
The University of Iowa
yannick-meurice@uiowa.edu

Lattice 2010, June 18, 2010

work done in part with Alexei Bazavov, Alan Denbleyker, Daping Du, Yuzhi "Louis" Liu, Alex Velytsky and Haiyuan Zou

Content of the talk

- Losing conformality=confinement=complex fixed points (Kaplan et al.)
- New picture: Fisher's zeros as boundary and gates for complex RG flows
- $2D$ $O(N)$ nonlinear sigma models
- Ising Hierarchical model ($D=$ 2 and 3)
- Fisher's zeros in $U(1)$ and $SU(2)$ LGT
- Conclusions

Outline in arXiv:1005.1993; PRL 104 or 105 (in press)

Conformality versus Confinement

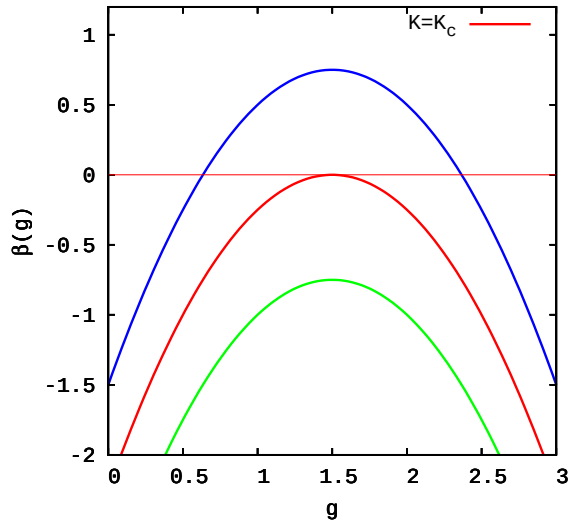

Figure 1: By reducing the constant term in a quadratic β function, the IR and UV fixed points merge and disappear in the complex plane, a mass gap is created, conformality is replaced by confinement (Kaplan, Son and Stephanov, PRD80)

Fisher's zeros as "gates" for complex RG flows

- Motivated by KSS observation, we studied complex extensions of RG flows in asymptotically free models where the weakly coupled flows reach the strongly coupled fixed point.

- We considered modifications or deformations that may affect that behavior (finite volume, change of dimension, additional pieces in the action).

- In all cases, the Fisher's zeros (of the partition function) seem to govern the global behavior of the flows near the real axis. It is plausible that in the infinite volume limit, these zeros delimit the boundary of the basin of attraction of the strongly coupled fixed point. For confining models, a "gate" remains open.

Models Considered

- $2D$ $O(N)$ non-linear sigma models in the large N limit.
- Ising hierarchical model $D = 2$ (no transition!) and 3 (usual Wilson fixed point). The probability distribution for the total spin in blocks of any size can be calculated exactly.
- $U(1)$ and $SU(2)$ $4D$ LGT (zeros at diferent volume; no RG flows yet).
- Models with fermions, in progress.

Note: at finite volume, these models have partition functions analytical in the entire complex β plane.

2D O(N) non-linear sigma model

$Z = \int \prod_{\mathbf{x}} d^N \phi_{\mathbf{x}} \delta(\vec{\phi}_{\mathbf{x}}.\vec{\phi}_{\mathbf{x}} - 1) \mathrm{e}^{-(1/g_0^2) \sum_{\mathbf{x},\mathbf{e}} (1 - \vec{\phi}_{\mathbf{x}}.\vec{\phi}_{\mathbf{x}+\mathbf{e}})}$

Notations: $\beta \equiv \frac{1}{(g_0^2 N)}$ (inverse 't Hooft coupling), $M \equiv \frac{m_{gap}}{\Lambda_{UV}}$

Large N: $\beta(M^2) = \int_{-\pi}^{\pi} \int_{-\pi}^{\pi} \frac{d^2k}{(2\pi)^2} \frac{1}{2(2 - \cos(k_1) - \cos(k_2)) + M^2}$

Infinite volume, small coupling (AF): $\beta(M^2) \simeq 1/(4\pi) \ln(1/M^2)$

Complex RG I: $m_{gap} = \epsilon \mathrm{e}^{i\theta}$ (small circle around 0), $\Lambda_{UV} \to \Lambda_{UV}/b$

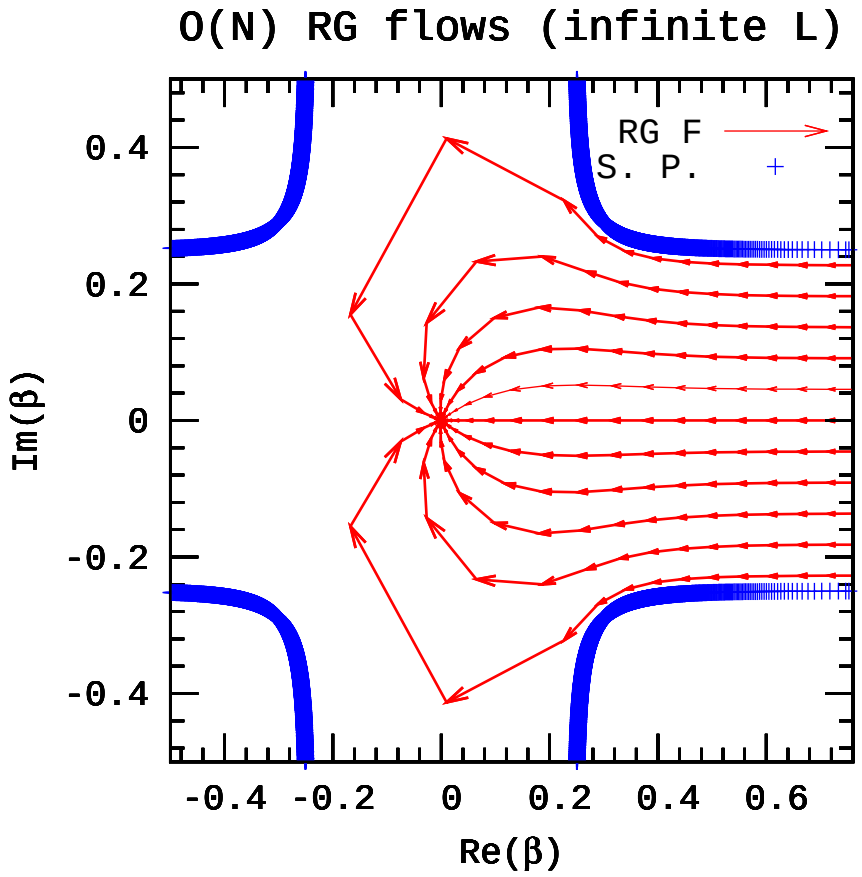

Figure 2: Infinite L RG flows (arrows). The blending blue crosses are the β images of two lines of points located very close above and below the $[-8, 0]$ cut of $\beta(M^2)$ in the M^2 plane.

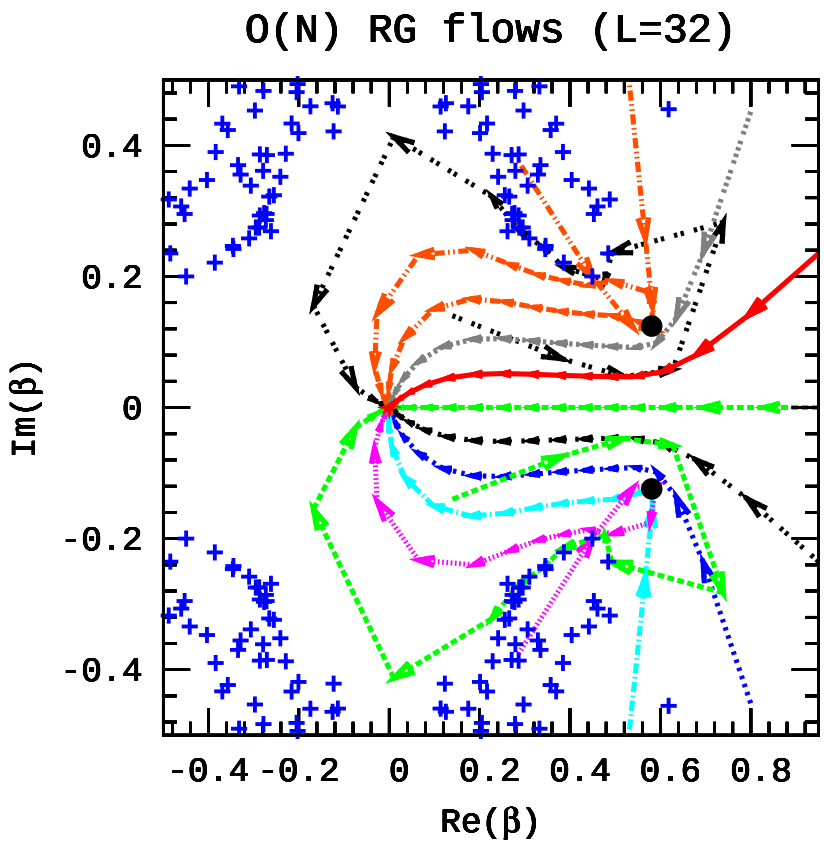

Figure 3: Same procedure and initial conditions but for $L = 32$. $\beta(M^2)$ is now a rational function; the crosses are the images of the singular points. The image of the two singular points closest to 0 appear as two large filled circles.

Complex RG II: Two-lattice matching

We consider the sums of the spins in four $L/2 \times L/2$ blocks B; NB is a nearest neighbor block of B. We define (possibly by reweighting):

$$R(\beta, L) \equiv \frac{\left\langle (\sum_{x \in B} \vec{\phi}_x)(\sum_{y \in NB} \vec{\phi}_y) \right\rangle_\beta}{\left\langle (\sum_{x \in B} \vec{\phi}_x)(\sum_{y \in B} \vec{\phi}_y)) \right\rangle_\beta} \ .$$

A discrete RG transformation mapping β into β' while the lattice spacing changes from a to $2a$ is obtained by matching: $R(\beta, L) = R(\beta', L/2)$.

Search with Newton's method: ambiguity$\equiv |\beta - \beta_{closest}|/|\beta - \beta_{2d.closest}|$

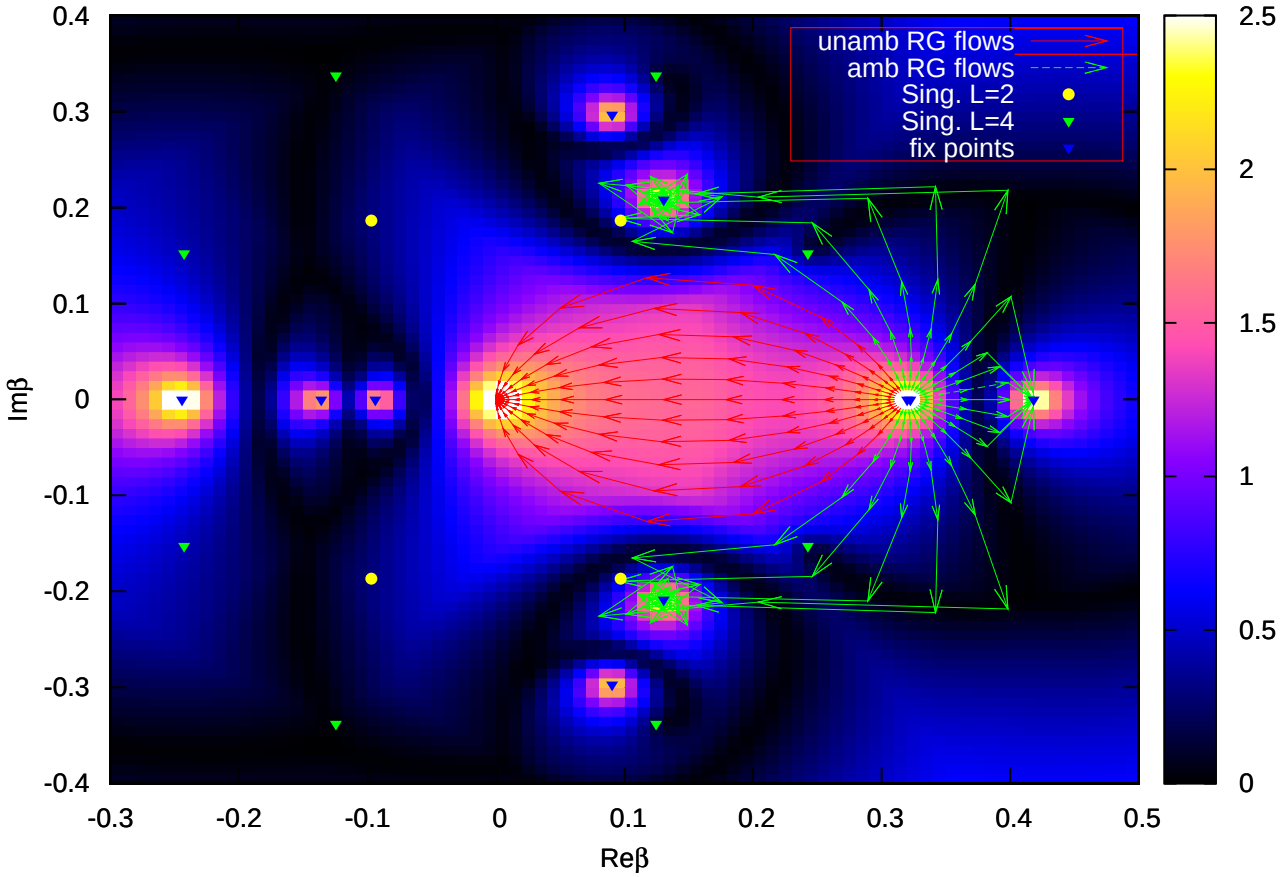

Figure 4: Complex RG flows $L = 4$; Color scale :-Ln(ambiguity)

Hierarchical Model

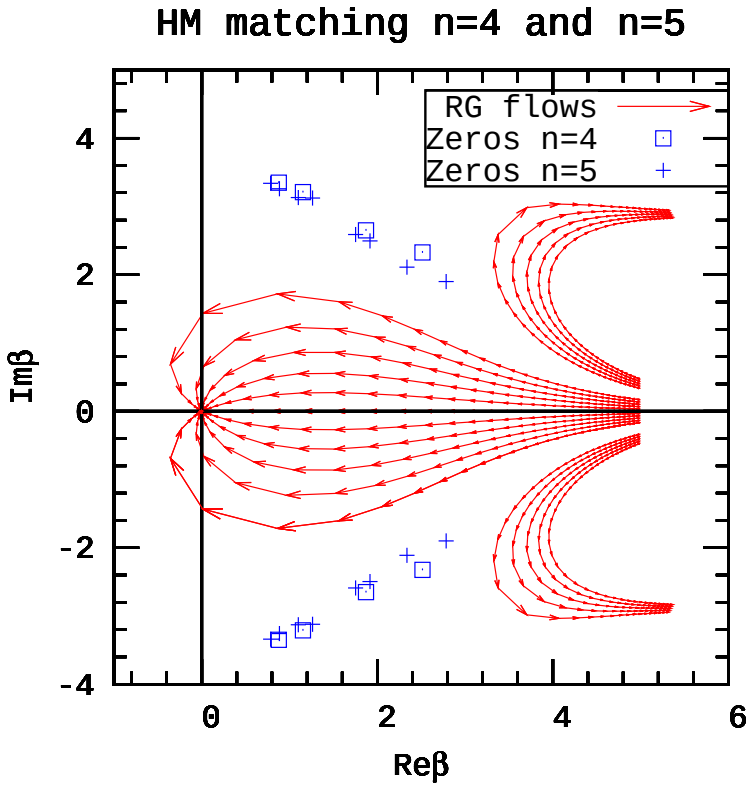

Figure 5: Unambiguous RG flows for the hierarchical model in the complex $\beta = 1/kT$ plane obtained by the two lattice method. The crosses and open boxes are at the Fisher's zeros for 2^4 and 2^5 sites.

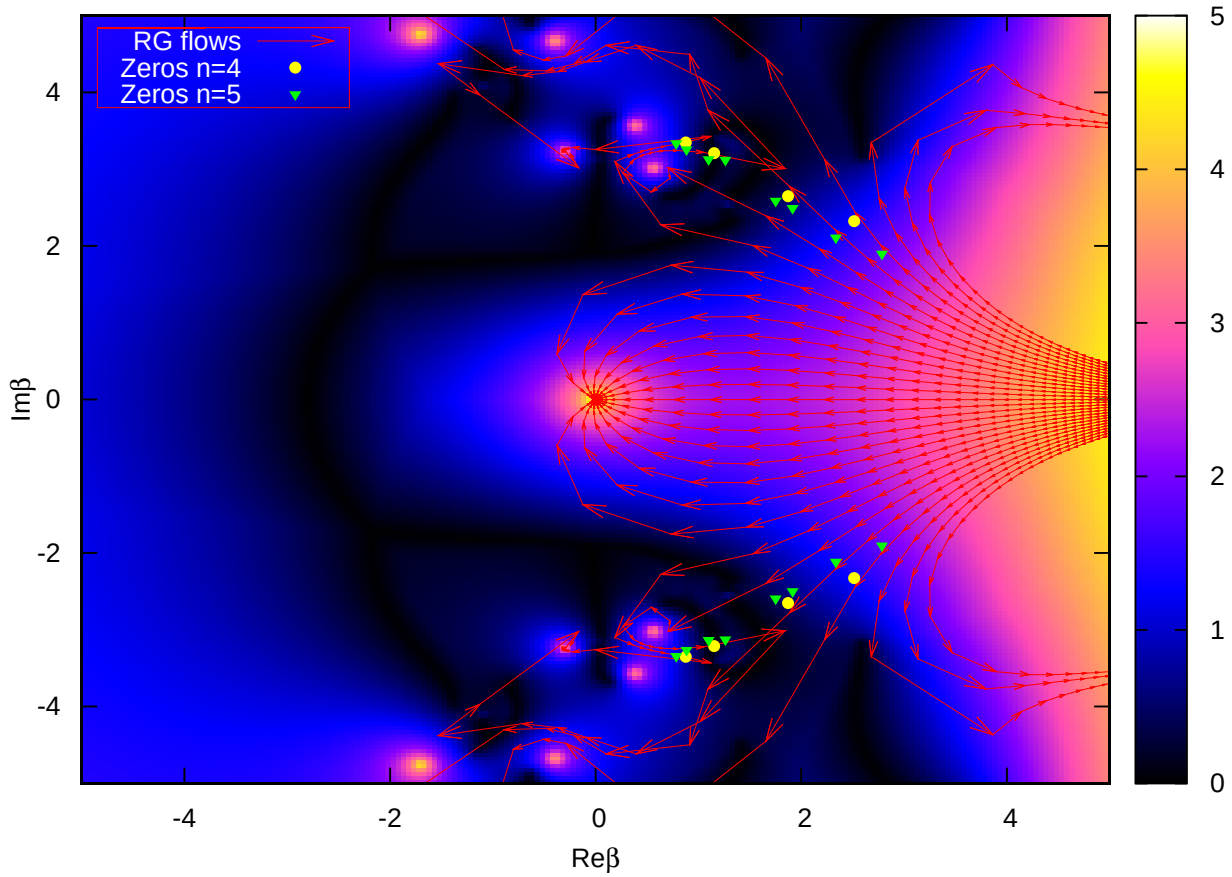

Figure 6: RG flows for the $D = 2$ hierarchical model in the complex β plane obtained by the two lattice method. Circles and triangles are at the Fisher's zeros for 2^4 and 2^5 sites. Darker=more ambiguous.

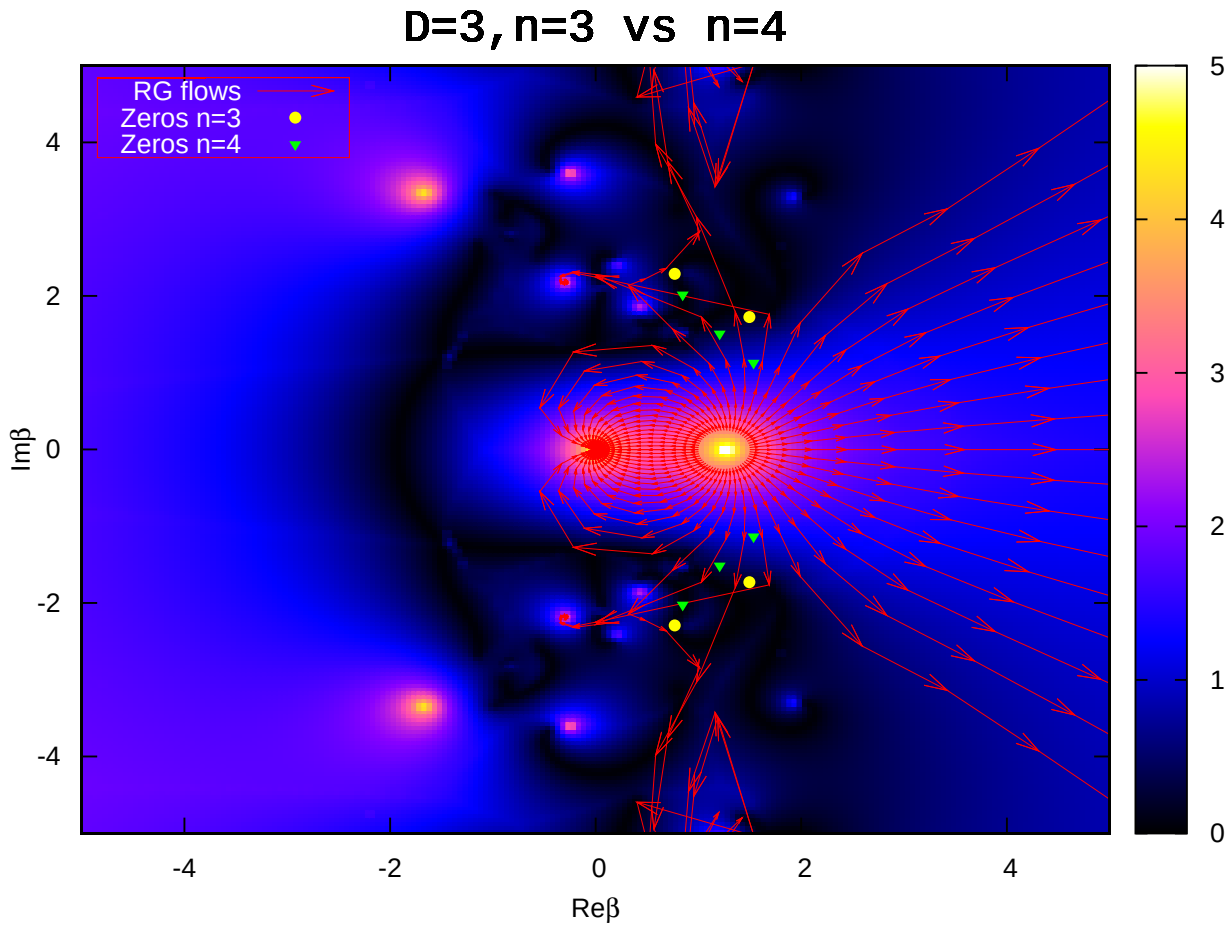

Figure 7: RG flows for the $D = 3$ hierarchical model in the complex β plane obtained by the two lattice method. Circles and triangles are at the Fisher's zeros for 2^3 and 2^4 sites. Darker=more ambiguous.

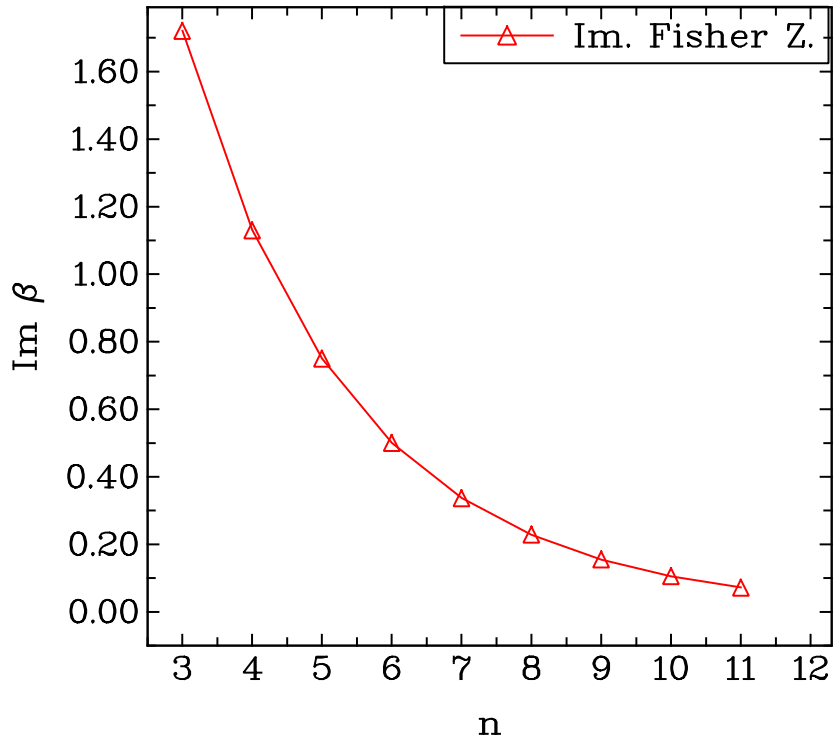

Figure 8: Imaginary part of the lowest Fisher's zero for the $D = 3$ hierarchical model for 2^n sites (the zeros pinch the real axis).

Fisher's zeros in $4D$ LGT

Spectral decomposition: $Z = \int_0^{S_{max}} dS n(S) \mathrm{e}^{-\beta S}$

$n(S)$: density of states; $\mathcal{N}$: number of plaquettes.

$n(S)\mathrm{e}^{-\beta \mathcal{N} s} = \mathrm{e}^{\mathcal{N}(f(s)-\beta s)} = \mathrm{e}^{\mathcal{N}(f(s_0)+(1/2)f''(s_0)(s-s_0)^2+\dots)}$

with $s = S/\mathcal{N}$ and $f'(s_0) = \beta$. $f(s)$ is a color entropy density.

If $Ref''(s_0) < 0$, the distribution becomes Gaussian in the infinite volume. Gaussian distributions have no complex zeros. The level curve $Ref''(s_0) = 0$ is the boundary of the region where Fisher's zeros may appear.

In the $U(1)$ case, conjugate pairs pinch the real axis, but for $SU(2)$ a finite gap remains present.

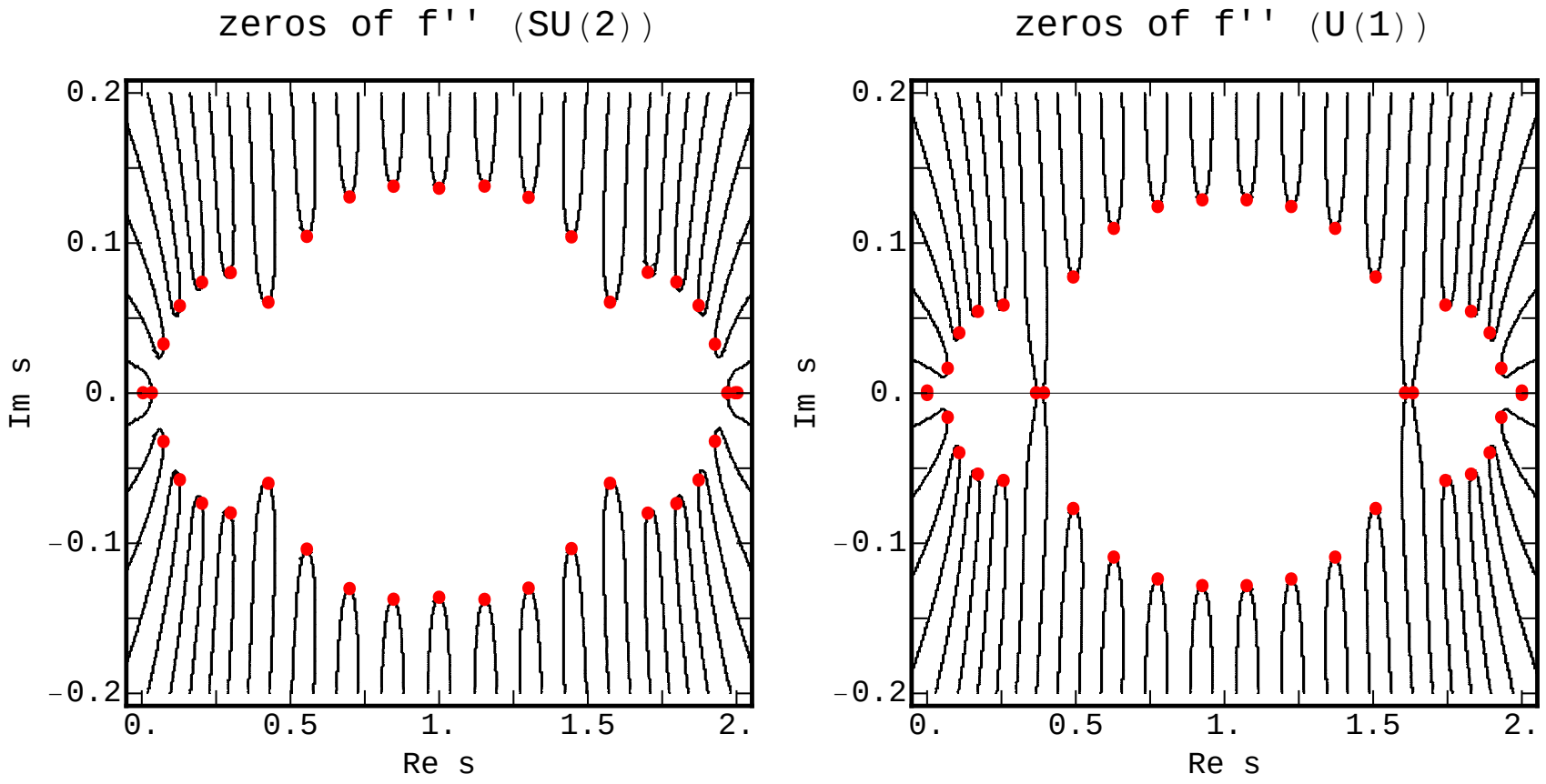

Figure 9: Complex zeros and zeros of the real part of $f''(s)$ in the complex s plane with a Chebyshev (40) on 4^4 for $SU(2)$ (left) and $U(1)$ (right).

These pictures suggest that Fisher's zeros should appear on approximately vertical linear structures. This is confirmed numerically.

For $U(1)$, naive histogram reweighting works well. δZ can be estimated from $(n_i(S) - < n(S) >)$, where i is an index for independent runs. Zeros can be excluded if $|\delta Z| << |Z|$.

For $SU(2)$, the imaginary part of Fisher's zeros are too large to use simple reweighting methods. By using Chebyshev interpolation for $f(s)$ and monitoring the numerical stability of the integrals with the residue theorem, it is possible to obtain reasonably stable results. Unlike the $U(1)$ case, the imaginary part of the lowest zeros does not decrease as the volume increases, but their linear density increases at a rate compatible with L^{-4}.

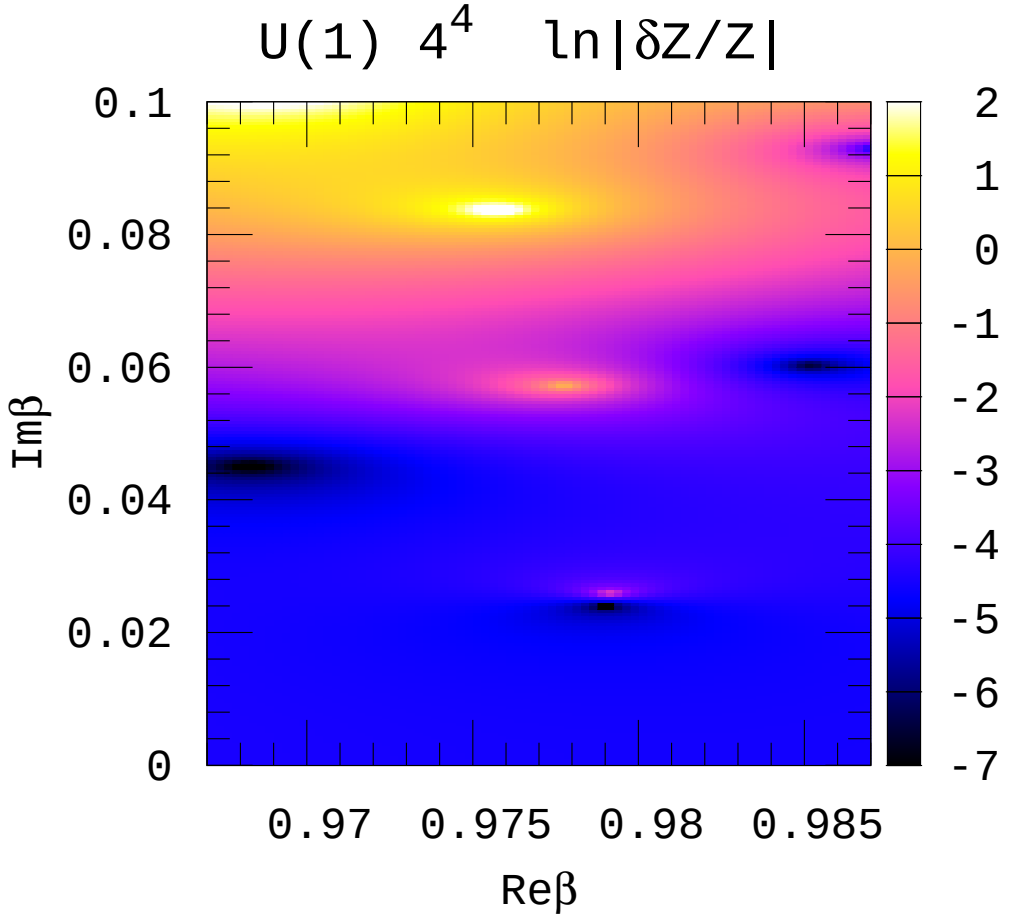

Figure 10: $|\delta Z/Z|$ for $U(1)$ on 4^4.

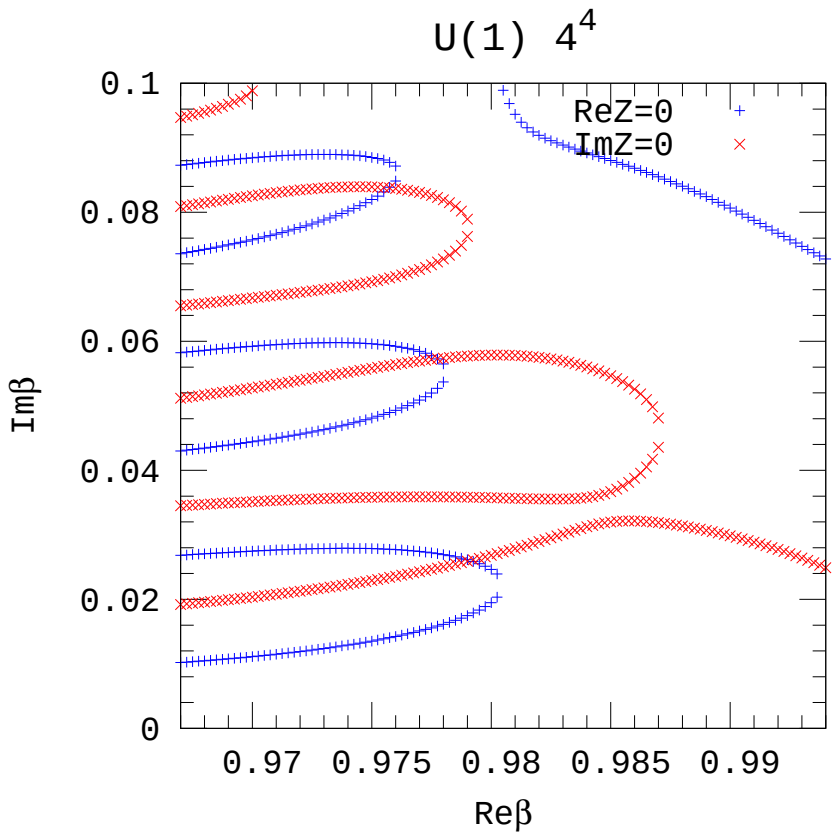

Figure 11: Zeros of the Re (blue) and Im (red) part of Z for $U(1)$ using the density of states for 4^4.

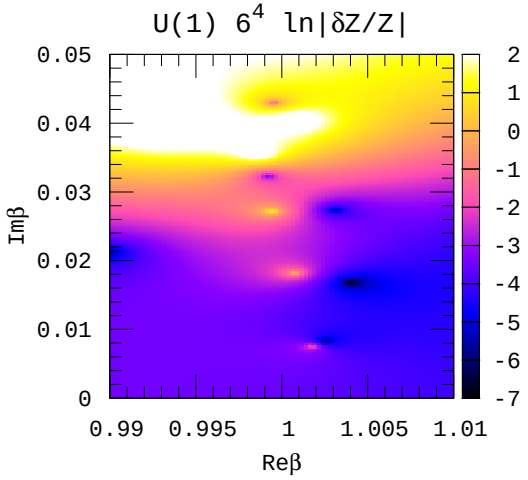

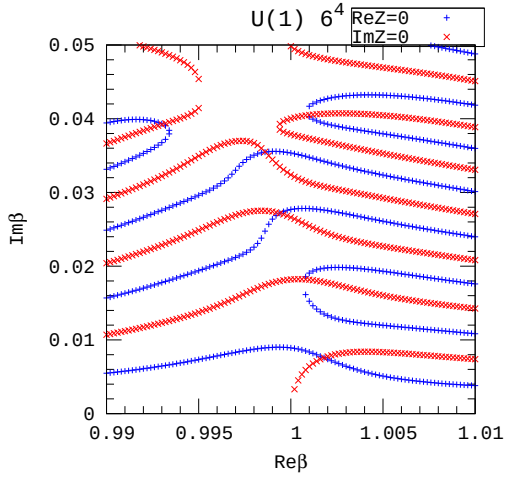

Figure 12: Same figures for a 6^4 lattice.

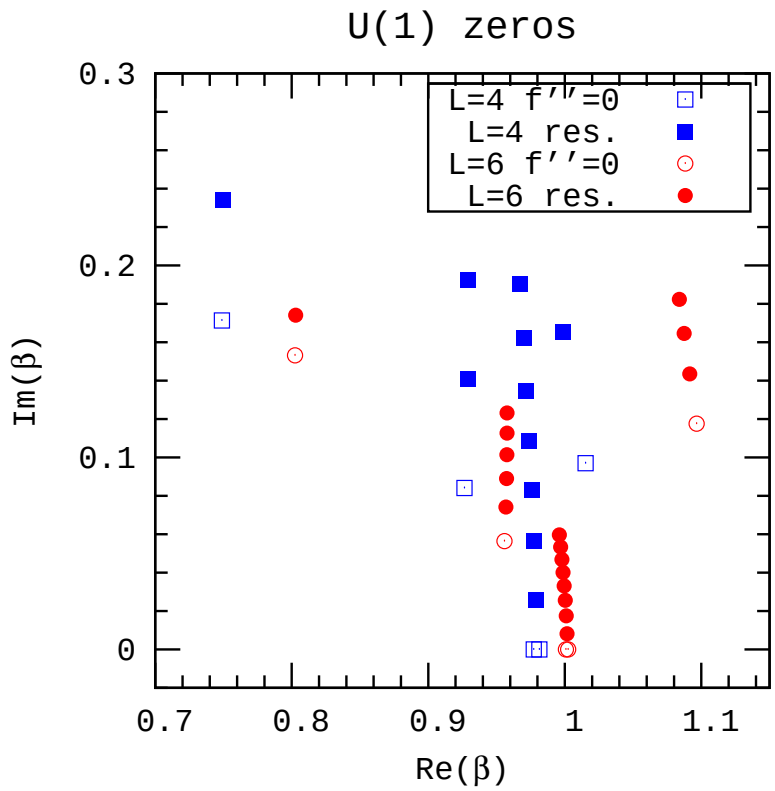

Figure 13: Images of the zeros of $f''(s)$ in the β plane (open symbols) and Fisher's zeros (filled symbols) for $U(1)$ on 4^4 (squares) and 6^4 (circles) lattices.

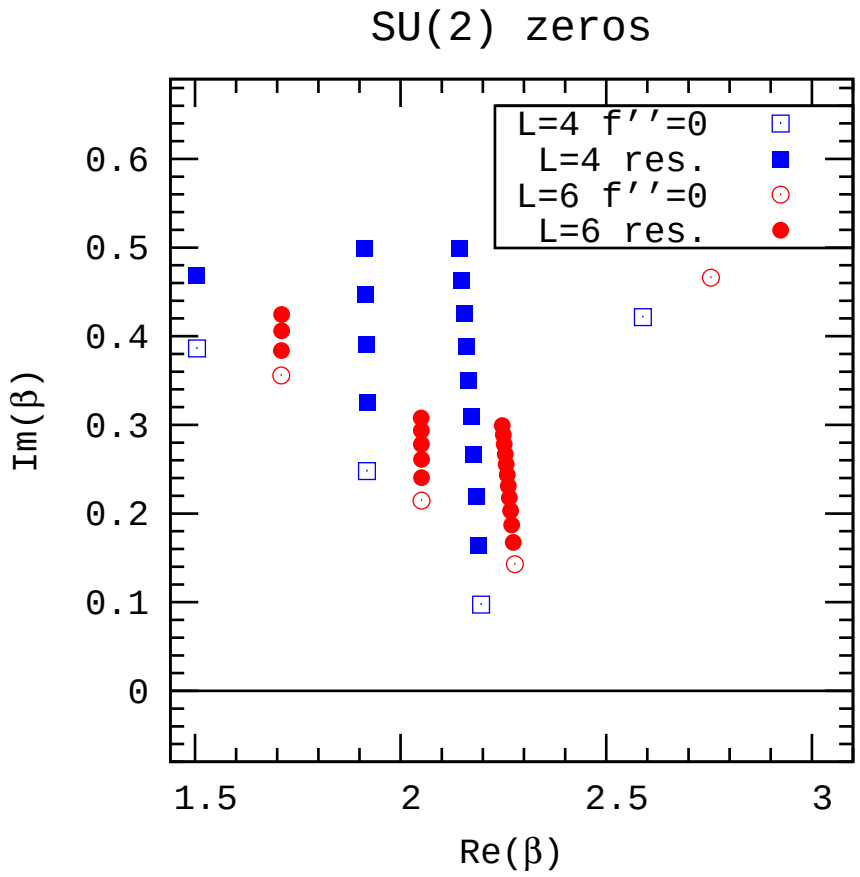

Figure 14: Images of the zeros of $f''(s)$ in the β plane (open symbols) and Fisher's zeros (filled symbols) for $SU(2)$ on 4^4 (squares) and 6^4 (circles) lattices.

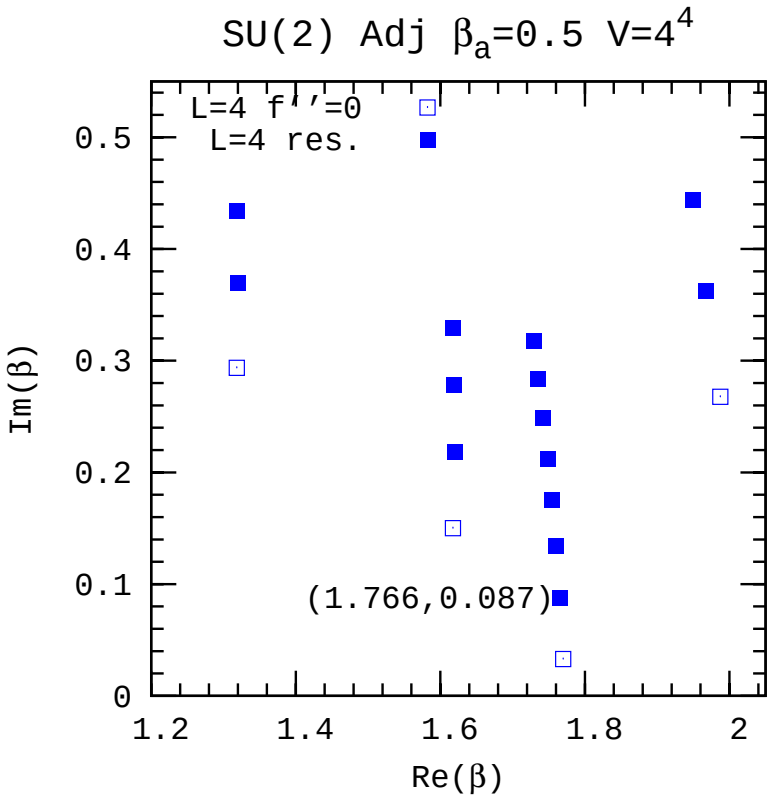

Figure 15: Effect of an adjoint term (+0.5), the lowest zero goes down by about 40 percent.

Conclusions

- It is possible to extend various RG flows to the complex β plane.
- When the size of the system is comparable to the Compton wavelength of the gap, there is a strong scheme dependence.
- Fisher's zeros control the global behavior of the RG flows.
- Confinement= "open gate".
- Plans: QED, $SU(3)$ with various N_f.
- Thanks!